Next-Generation Chip Scale Atomic Clocks

John Kitching, Matt Hummon, William McGehee, Ying-Ju Wang, and Susan Schima

Time and Frequency Division, National Institute of Standards and Technology, MS 847, 325 S. Broadway, Boulder CO 80305

john.kitching@nist.gov

Abstract. We describe three independent research directions focussed on the development of next-generation chip-scale atomic clocks, which combine small size, low power consumption and manufacturability with high frequency stability. The use of optical transitions in microfabricated vapor cells improves both short- and long-term frequency stability to near 10^{-13} at the cost of the added complexity of a chip-scale optical frequency comb. Chip-scale atomic beam microwave clocks have been successfully demonstrated and offer the potential for microsecond-level timing accuracy over one week. And finally, Sr vapor cells have been developed with lifetimes exceeding 250 hours and residual gas pressures below 1 Torr.

1. Introduction

Chip scale atomic clocks [1-3], developed throughout the 2000s and released as a product in 2011 [7], have surpassed 95,000 units in sales [9] and have established themselves as a significant component of the commercial atomic timing market. With a power consumption of under 200 mW and a timing stability of 1 μs over 1 day under controlled environmental conditions [7], this unique combination of properties enables their use in application spaces where GPS is unavailable and battery operation is needed. Chip-scale atomic clocks are finding widespread use in underwater timing for oil and gas exploration [10,11], have been flown in space [12,13] and can improve the performance of satellite-based navigation systems [14,15]. Efforts are underway to reduce production cost, potentially enabling use in an even broader set of applications.

The key technical elements of these clocks are the use of silicon micromachining to fabricate the vapor cell [16], a low-power diode laser as the light source [17] and a thermal suspension system to isolate the physics package from the environment [18]. Together, these elements allow clock operation with significantly lower power consumption [19] than is possible in conventional designs [20].

The commercial success of this technology, as well as new applications requiring a higher level of timing precision, has motivated the search for improvements across a range of parameters, but most importantly in the long-term stability. Chip-scale atomic clocks exhibit a fractional frequency drift of up to $3 \times 10^{-10}/\mathrm{mo}$ [7], limiting their use in applications where accurate time is required over extended periods. In addition, vapor cell clocks possess no intrinsic frequency accuracy due to the large shift of the clock frequency created by the presence of the buffer gas. Periodic recalibrations are therefore required to maintain timing accuracy.

In this Proceedings, we review efforts in our group over the last few years to develop next-generation chip-scale atomic clocks that retain compact form factors, low power consumption and a high degree of

manufacturability while simultaneously achieving improved frequency stability, especially over long integration times. Compact optical clocks [5,8,21] have been demonstrated based on the two-photon optical transition in Rb at 778 nm, which incorporate microresonator frequency combs to divide the optical frequency down to the microwave domain. A microfabricated microwave atomic beam clock was also developed that shows promise for microsecond-level timing stability over one week. Finally, we have demonstrated Sr vapor cells, with lifetimes exceeding several hundred hours at elevated temperature.

2. Compact optical clocks

Following the development of the optical frequency comb in the late 1990s and early 2000s [22], tremendous progress has been made in the field of optical clocks, which now achieve fractional frequency uncertainties near 10^{-18}, a factor of 100 better than the best microwave clocks [23]. This improvement is largely driven by the ~ 10^5 × larger carrier frequency, which leads to correspondingly higher resonance quality factors. Optical frequency combs have been implemented using Kerr nonlinearities in on-chip whispering-gallery mode optical resonators [24,25], which has opened the door to the possibility of chip-scale optical clocks.

The two-photon (2-hv) transition in Rb at 778 nm has been investigated for many decades [26-29] as a high-performance optical frequency reference and is identified by the BIPM as a secondary representation of the SI meter [30]. This transition has the advantages of a reasonably narrow linewidth (300 kHz), a small light shift, and accessibility in a simple vapor cell configuration.

2.1. A compact 2-hv optical clock

A compact Rb 2-hv optical clock using a pair of toroidal microresonator frequency combs is shown in Fig. 1(a) [5]. The Rb 2-hv transition is excited using a distributed Bragg reflector laser at 778 nm. The resonance is detected by monitoring the 420 nm fluorescence generated by the atoms decaying to their ground state via a cascade transition through the $6P_{3/2}$ level (see Fig. 1(b)). Locking the DBR laser to the 2-hv transition generated a short-term frequency stability on the optical reference of $4.4 \times 10^{-12}/\sqrt{\tau}$, with a flicker floor near 10^{-13}, as shown in Figure 1(c).

The frequency division is accomplished using two microresonator combs: a small Si_3N_4 resonator driven at 1540 nm produces an octave-spanning comb with a spacing of 1 THz that is self-referenced to control the carrier offset frequency; and a larger SiO_2 resonator driven at 1556 nm produces a comb with a mode spacing of 22 GHz, which spans the frequency gap between two adjacent comb teeth in the 1 THz comb. Phase locks between the comb teeth stabilize the carrier envelope offset frequency for the comb pair. A phase lock of one comb tooth to the Rb DBR laser allows coherent division of the atomically stabilized light at 778 nm down to 22 GHz without adding any additional instability as shown by the overlap of the microwave and optical reference data points in Fig. 1(c).

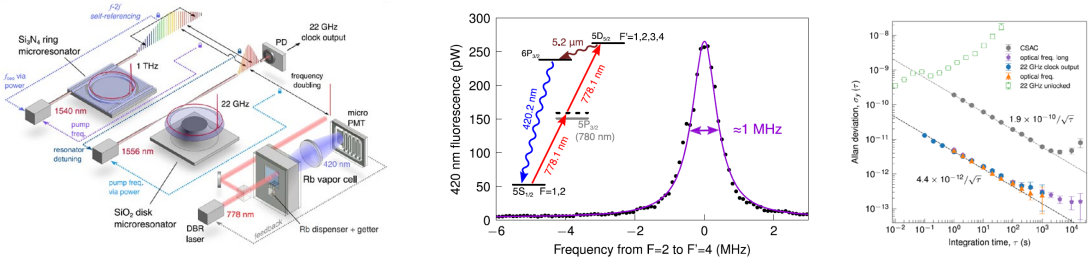

(a) (b) (c)

Fig. 1 (a) Chip-scale optical clock incorporating a Rb 2-hv optical reference and a pair of microresonator optical frequency combs to perform the frequency division. (b) Fluorescence signal from Rb 2-hv optical reference. (c) Allan deviation of the chip-scale optical clock compared to a conventional (microwave) chip-scale atomic clock. (From Ref. [5])

Full integration and manufacturability of such optical clocks is a major remaining challenge. The clock optics require multiple materials platforms, Si_3N_4, SiO_2, and InGaAsP if the lasers are to be included on-chip, as well as frequency doubling capability. Substantial optical power from the lasers may also be required (100 mW at 1540 nm and 160 mW at 1556 nm) due to losses associated with coupling light on and off the chips. In addition, a more highly integrated Rb 2-hv reference would need to be developed, perhaps using photonic integrated circuits [31].

2.2. High-performance 2-hv optical reference

The short-term stability of the optical clock in the previous section was limited by intermodulation effects, in which FM noise on the DBR laser at twice the FM modulation frequency used to lock the laser is coupled down to DC. By replacing the DBR laser with an extended-cavity laser with a narrower linewidth, this source of instability could be suppressed as shown in Fig. 2 [8]. In this case, the short-term instability could be reduced to $1.8 \times 10^{-13}/\sqrt{\tau}$, with about half of this instability coming from photon shot noise and the other half due to the intermodulation effect. A flicker floor below 2×10^{-14} was observed out to an integration time of one hour.

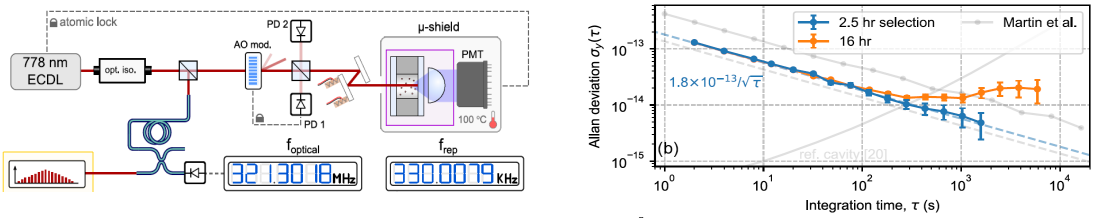

(a) (b)

Fig. 2 (a) Rb 2-hv optical clock operated with an external cavity laser. (b) improved short-term frequency stability is obtained compared to operation with a DFB laser due to the reduction of intermodulation instability caused by laser FM noise. (From Ref. [8])

3. Chip-scale atomic beam clocks

Atomic beam clocks have been a workhorse in precision timing since the 1950s [32,33] and commercial versions of these with beam tube lengths on the order of 15 cm achieve accuracies below 10^{-12} and long-term stabilities below 10^{-13}. Such a clock, if implemented at the chip scale with low power consumption, could therefore be an ideal complement to chip-scale vapor cell clocks even with the degraded stability and accuracy implied by the shorter tube length.

3.1. Clock design

A chip-scale atomic beam clock physics package is shown in Fig 3 [4]. The device is 25 mm in length, 19 mm wide and 5 mm thick, and contains a source region containing a thermal vapor of Rb, channels etched in silicon to create a collimated beam [34], and drift region in which the atoms are interrogated. Rb is created in the source region from a Rb_2MoO_4/AlZr pill activated to produce elemental Rb by a high-power laser after the chamber is sealed [35]. Non-evaporable getters pump most gases in the drift region and graphite is used to reduce the background Rb gas pressure in the drift region. The beam flux at a temperature of 90 °C is approximately 5×10^{11} at/s at the output of the collimator.

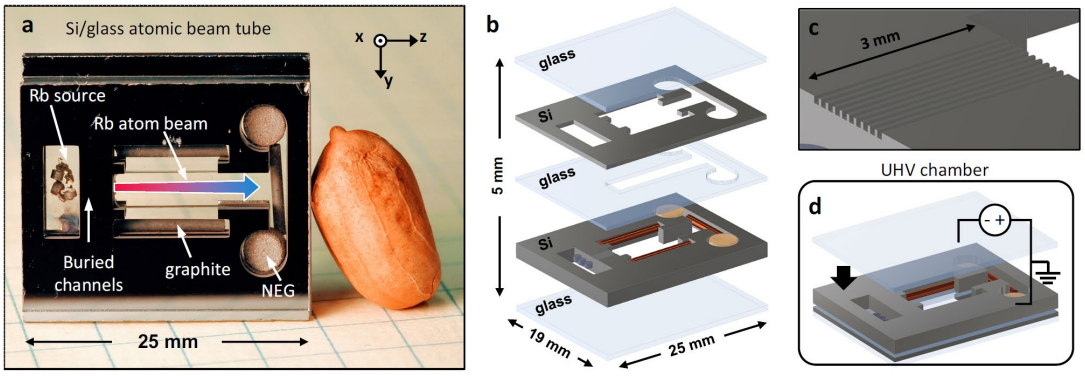

Fig. 3 (a) Chip-scale atomic beam clock photograph showing the Rb source region and the atomic beam propagation direction. (b) Device structure. (c) Channels etched in Si that collimate the atomic beam. (d) Fabrication process in which glass is anodically bonded to the top silicon surface to form an evacuated package. (From Ref. [4])

3.2. Frequency stability

Atoms in the atomic beam are excited using Ramsey coherent population trapping [36,37]. The atomic florescence detected in the second Ramsey zone shows typical thermal beam Ramsey fringes with a width of 12 kHz, as shown in Fig. 4(a), determined by the transit time of the atoms between the zones. Stabilization of a microwave oscillator using this signal results in a sort-term instability of $1.2 \times 10^{-9}/\sqrt{\tau}$ out to 100 s, as shown in Fig. 4(b). While this stability is quite poor (worse even than the stability of a commercial chip-scale atomic clock), significant improvements are anticipated with future work, for example, through improving the collection efficiency of the florescence light. It is expected that the long-term stability at integration times beyond one day, will be considerably better than a vapor cell CSAC if systematic effects such as the AC Stark shift and Rb-Rb collision shift can be adequately controlled.

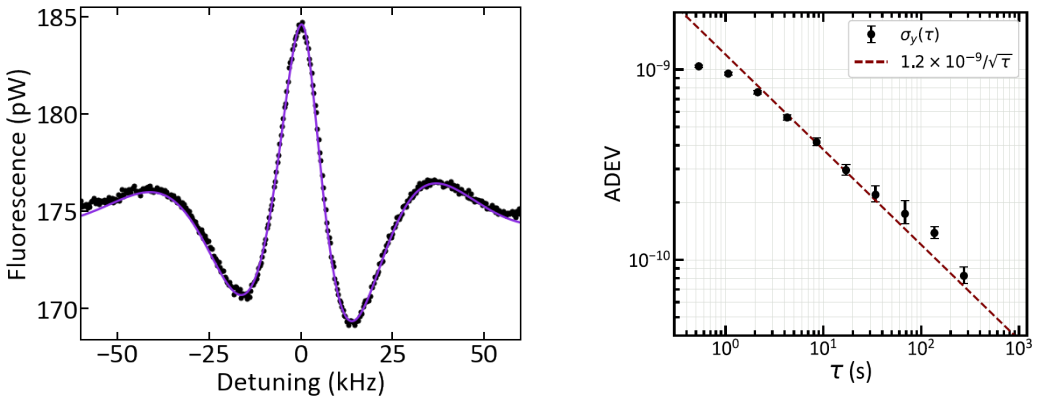

Fig. 4 (a) Ramsey fringes generated by coherent population trapping in a microfabricated atomic beam clock with a Ramsey zone of 1 cm. (b) Clock stability. (From Ref. [4])

4. Strontium vapor cells

Alkaline earth atoms are of high interest for optical frequency references due to the long coherence times of some transitions in these species. These atoms are the basis for some of the most stable and accurate optical lattice clocks currently under development [23]. Alkaline earth atoms have transitions that span

a broad range of linewidths, from several tens of megahertz to the millihertz range. This makes them interesting for references based on vapor cell or atomic beams [38], where transit time broadening in centimetre-scale geometries results in minimum linewidths in the range of 10 kHz - 100 kHz. The low vapor pressure of alkaline earth atoms means that temperatures near 300 °C are required for optical thicknesses approaching unity. At this elevated temperature alkaline earth atoms are known to damage most glasses typically used as windows. As a result, fairly complex experimental systems such as hollow cathode lamps or heat pipes are traditionally used.

4.1. Cell fabrication

Sr vapor cells, shown in Fig. 5(a) were fabricated using anodic bonding processes similar to those used to make alkali vapor cells. The interior windows of the cell were coated with Al_2O_3 [39] to prevent interaction of the Sr with the glass as shown in Fig. 5(b). Sr metal was inserted into the cell cavity in a dry nitrogen environment and the filled cavity was quickly transferred into an anodic bonding system, which was subsequently evacuated for sealing under vacuum.

4.2. Absorption spectroscopy

After fabrication, absorption spectroscopy was carried out at temperatures above 300 °C to confirm the presence of Sr vapor in the cell. A typical absorption line in a counterpropagating geometry is shown in Fig. 5(c). A key question is the extent to which the Al_2O_3 coating protects the cell windows over extended periods. This was assessed by measuring the transmission through the vapor cell (at 461 nm) over many days; when alkaline earth atoms react with the glass walls, the glass becomes opaque, and the optical transmission is reduced. No measurable change in the transmission was observed over 250 hours at a temperature above 300 °C.

The width of the narrow Doppler-free feature near the line centre was used to assess the pressure of residual gases in the cell, since such gases broaden optical transitions in alkaline earth atoms. By measuring the linewidth of the transition at 461 nm as a function of optical power, and extrapolating to zero power, an upper limit on the residual gas pressure was established of ~ 50 Pa (0.4 Torr), consistent with zero. Further measurements on narrower transitions (for example of the 7.5 kHz-wide transition at 689 nm) are expected to provide more stringent limits on the presence of any residual gas.

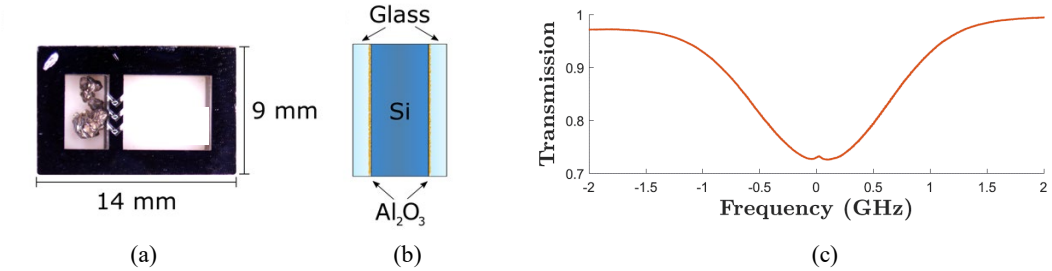

Fig. 4 (a) Photograph of a microfabricated Sr vapor cell. (b) Cell design: Al_2O_3 coatings on the interior surfaces of the vapor cell protect the cell windows from the corrosive Sr vapor. (c) Absorption spectrum at 461 nm at a temperature near 320 °C with counterpropagating optical fields. A Doppler-free feature is observed at the line centre. (From Ref. [6])

5. Conclusion

Next-generation chip-scale atomic clocks based on optical transitions in atoms or atomic beams promise improved frequency stability at both short and long integration times while retaining the low power consumption and manufacturability of the original technology. The proof of principle demonstrations of such clocks described here provide a foundation for future work to enhance the engineering and manufacturing maturity. While considerable work is still needed to achieve product prototypes,

especially with regard to thermal engineering for low power consumption, such clocks would likely make considerable impact on real-world applications if successfully commercialized.

References

[1] Knappe S, Shah V, Schwindt P D D, Hollberg L, Kitching J, Liew L A, and Moreland J 2004 *Appl. Phys. Lett.* **85**, 1460
[2] Lutwak R et al. 2007 *Proc. Precise Time and Time Interval (PTTI) Meeting*, Long Beach, CA, 269
[3] Kitching J 2018 *Applied Physics Reviews* **5**, 031302
[4] Martinez G D, Li C, Staron A, Kitching J, Raman C, and McGehee W R 2023 *Nat. Commun.* **14**, 3501
[5] Newman Z L et al. 2019 *Optica* **6**, 680
[6] Pate J M, Kitching J, and Hummon M T 2023 *Opt. Lett.* **48**, 383
[7] Lutwak R 2011 *Proc. Precise Time and Time Interval (PTTI) Meeting*, Long Beach, CA, 207
[8] Newman Z L, Maurice V, Fredrick C, Fortier T, Leopardi H, Hollberg L, Diddams S A, Kitching J, and Hummon M T 2021 *Opt. Lett.* **46**, 4702
[9] Cash P, Krzewick W, Machado P, Overstreet K R, Silveira M, Stanczyk M, Taylor D, and Zhang X 2018 *Proc. 2018 European Frequency and Time Forum (EFTF)*, 65
[10] Gardner A T and Collins J A 2012 *Proc. MTS/IEEE Oceans Conference*, Hampton Roads, VA, 1
[11] Gardner A T and Collins J A 2016 *Proc. MTS/IEEE Oceans Conference*, Monterey, CA, 1
[12] Lezius M et al. 2016 *Optica* **3**, 1381
[13] CAPSTONE Mission, 2023 https://advancedspace.com/capstone-30aug23-update/
[14] Krawinkel T and Schön S 2015 *Proc. ION GNSS*, 2867
[15] Krawinkel T and Schon S 2016 *GPS Solutions* **20**, 687
[16] Liew L A, Knappe S, Moreland J, Robinson H, Hollberg L, and Kitching J 2004 *Appl. Phys. Lett.* **84**, 2694
[17] Chantry P J, Liberman I, Verbanets W R, Petronio C F, Cather R L, and Partlow W D 1996 *Proc. IEEE Int. Freq. Cont. Symp.*, 1002
[18] Mescher M J, Lutwak R, and Varghese M 2005 *Proc. Solid-State Sensor, Actuator and Microsystems Workshop*, Seoul, Korea, 311
[19] Lutwak R et al. 2004 *Proc. Precise Time and Time Interval (PTTI) Meeting*, Washington, DC, 339
[20] Vanier J and Audoin C 1992 *The Quantum Physics of Atomic Frequency Standards* (Bristol: Adam Hilger)
[21] Maurice V et al. 2020 *Opt. Exp.* **28**, 24720
[22] Diddams S A et al. 2000 *Phys. Rev. Lett.* **84**, 5102
[23] Ludlow A D, Boyd M M, Ye J, Peik E, and Schmidt P O 2015 *Rev. Mod. Phys.* **87**, 637
[24] Del'Haye P, Arcizet O, Schliesser A, Holzwarth R, and Kippenberg T J 2008 *Phys. Rev. Lett.* **101**
[25] Kippenberg T J, Holzwarth R, and Diddams S A 2011 *Science* **332**, 555
[26] Cagnac B, Grynberg G, and Biraben F 1973 *J. Phys.* **34**, 845
[27] Poulin M, Latrasse C, Cyr N, and Tetu M 1997 *Phot. Tech. Lett.* **9**, 1631
[28] Edwards C S, Barwood G P, Margolis H S, Gill P, and Rowley W R C 2005 *Metrologia* **42**, 464
[29] Burke J, in *SPIE Photonics West* (San Francisco, 2016).
[30] Felder R 2005 *Metrologia* **42**, 323
[31] Hummon M T et al. 2018 *Optica* **5**, 443
[32] Vanier J and Audoin C 2005 *Metrologia* **42**, S31
[33] Essen L and Parry V I 1955 *Nature* **176**, 280
[34] Li C, Chai X, Wei B, Yang J, Daruwalla A, Ayazi F, and Raman C 2019 *Nat. Commun.* **10**, 1831

[35] Douahi A, Nieradko L, Beugnot J C, Dziuban J, Maillote H, Guerandel S, Moraja M, Gorecki C, and Giordano V 2007 *Elec. Lett.* **43**, 279
[36] Thomas J E, Hemmer P R, Ezekiel S, Leiby C C, Picard R H, and Willis C R 1982 *Phys. Rev. Lett.* **48**, 867
[37] Hemmer P R, Shahriar M S, Lamelarivera H, Smith S P, Bernacki B E, and Ezekiel S 1993 *J. Opt. Soc. Am. B* **10**, 1326
[38] Olson J, Fox R W, Fortier T M, Sheerin T F, Brown R C, Leopardi H, Stoner R E, Oates C W, and Ludlow A D 2019 *Phys. Rev. Lett.* **123**, 073202
[39] Woetzel S, Talkenberg F, Scholtes T, Ijsselsteijn R, Schultze V, and Meyer H G 2013 *Surf. Coat. Tech.* **221**, 158